

WAVE BREAKING AS PARTICLE “ESCAPE”: COMPARISONS WITH EXACT COMPUTATIONS

R.C.T. Rainey WS Atkins Oil & Gas, Euston Tower, London NW1 3AT, U.K. rod.rainey@atkinsglobal.com

SUMMARY

At the 2002 Workshop, the author proposed [1] a new theory of wave breaking. It is that breaking is not caused by an instability, as previously thought, but is a reflection of a type of singularity in the linear velocity field. The singularity may be detected by tracking a sheet of particles (or indeed a single particle) as they move in this velocity field – when they reach such a singularity, the particles “escape”.

This present paper presents comparisons between the threshold of particle “escape”, and the actual threshold of wave breaking as found by an exact fully-nonlinear computation. In the simple case of two waves of equal steepness ka , one twice as long as the other, an “escape” first occurs at $ka = 0.17$, or $ka = 0.21$ if the second-order potential is included. With the fully-nonlinear computation, the threshold of breaking is $ka = 0.18$.

1. BACKGROUND

When it is breaking, a wave often imparts a very much larger force on a ship or offshore structure. This can be because the acceleration under the crest is much higher than just before breaking – typically 5g rather than 0.5g, see New et al [2]. Or, it can be because the near-vertical face of the wave produces an impact. Whatever the mechanism, it is often the case that conventional predictions of wave load have to be thrown out of the window, and ship designers have to fall back on age-old empiricism.

For many years it has been widely believed that the origin of wave breaking is an instability of the wave crests. At the 2002 Workshop, however, the author proposed [1] a much simpler explanation, which is that breaking is a reflection of a type of singularity in the linear velocity field. The argument is laid out in full detail in [3]. No additional approximation is required to reveal the singularity. It is just a matter of replacing the classical arbitrary assumption with another equally valid one. The classical arbitrary assumption is that the theory of water waves should be based on a consideration of the zero-pressure surface, i.e. the dynamic boundary condition should be applied before the kinematic one. The alternative arbitrary assumption is that the kinematic boundary condition should be applied before the dynamic one. This means that the surfaces to be considered are not the constant-pressure surfaces, but are sheets of particles, moving in the velocity field defined by the first (or N th) order velocity potential. These satisfy the kinematic boundary condition exactly, just as the traditional constant-pressure surfaces satisfy the dynamic boundary condition exactly.

There is no change in the N th order boundary conditions on the still-water position $z = 0$, derived by such an alternative argument. The difference is in the underlying behaviour of the constant-pressure and particle-sheet surfaces, at finite wave steepness. The former are completely smooth and single-valued, suggesting that the explanation for wave breaking must be something quite outside the classical theory, such as an instability. By

contrast, the particle-sheet surfaces occasionally exhibit violent eruptions, with the particles escaping to infinity in finite time, and producing an overturning of the surface. This is a natural explanation for wave breaking, bringing it within the classical theory. It also applies to the case of wave diffraction around a body, and predicts for example wave breaking around a vertical cylinder, see the author’s paper [4] with J.R.Chaplin at the 2003 Workshop, which compares the results with experiments.

In the discussion of that paper, M.P.Tulin emphasised [5] the importance of checking the thresholds of wave breaking in the simpler case of undisturbed waves, by comparing with an exact non-linear computation. This present paper presents such comparisons, which are also featured in [3] and use the fully-nonlinear program from [2] which is described in detail by Dold [6].

2. PRELIMINARY CHECKS

A suitable case for exact computation is a pair of waves, one of twice the length of the other, and both of the same steepness ka . The computations can be started with the trough of the short wave coinciding with the crest of the long wave, and then run until the crests coincide, at which point (or close to it) the waves may break. The threshold of breaking, in terms ka , can readily be found, and compared with the threshold of particle “escape”. As usual with comparisons between two computer programs, great care is needed with the preliminary checks, to ensure compatibility between the two results.

We can take the first-order wave elevation as:

$$a_1 \cos(k_1 x - \omega_1 t) + a_2 \cos(k_2 x - \omega_2 t) \quad (1)$$

where in our case $k_1 = 2k_2$. We will set the scale by choosing $k_1/2 = k_2 = 1\text{m}^{-1}$ (i.e. wavelengths of π and 2π) and $g = 9.81\text{ m/s}^2$. The first order velocity potential associated with (1) is:

$$\frac{a_1 \omega_1}{k_1} e^{k_1 z} \sin(k_1 x - \omega_1 t) + \frac{a_2 \omega_2}{k_2} e^{k_2 z} \sin(k_2 x - \omega_2 t) \quad (2)$$

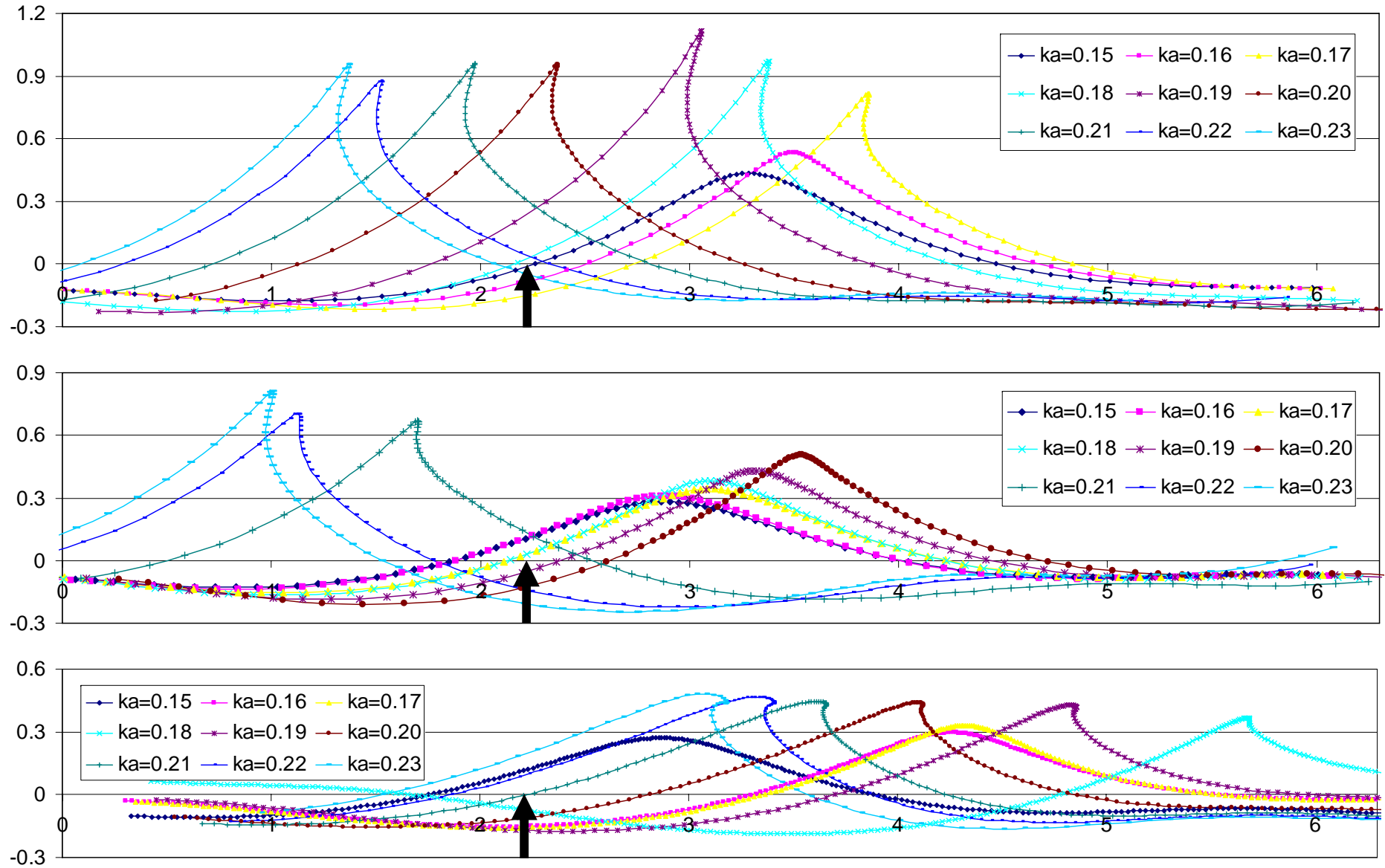


FIGURE 1. Particle-sheet surfaces based on 1st order flow (top) and 1st+2nd order flow (centre), together with an exact computation based on 2nd order starting conditions (bottom). The horizontal axis spans one wavelength (2π) of the longer wave. The crest of the longer wave and the trough of the shorter wave are both at π at the start of the computations. The particle sheets are shown at maximum crest elevation, or where they first overturn. The exact computations are shown at maximum crest elevation, or the farthest point reached by the program. The nominal focus point, where the crests coincide on classical 1st or 2nd order theory, is shown with an arrow.

Given that $k_1 > k_2$ the second order potential is:

$$-a_1 a_2 \omega_1 e^{(k_1 - k_2)z} \sin\{(k_1 - k_2)x - (\omega_1 - \omega_2)t\} \quad (3)$$

see e.g. Longuet-Higgins and Stewart [7].

To check that these potentials have been correctly programmed into MATHCAD, we can find the zero-pressure surface (by means of the Newton-Raphson scheme, using the full pressure formula) for very small values of ka . We can then place particles on it at the time when the trough of the short wave coincides with the crest of the long wave, follow them in the flow field defined by (2) + (3) until the crests coincide, and then find the pressure error on them. If (2) + (3) is indeed a correct second-order solution, this pressure error should be third order in ka . Likewise, if we omit (3) then these pressure errors should all be second order. The Table below gives the results (expressed as a vertical distance, i.e. a pressure head) in both cases.

ka	1 st order	2 nd order
0.1	3.4×10^{-2}	5×10^{-3}
0.01	2.6×10^{-4}	3.2×10^{-6}
0.001	2.6×10^{-6}	3.3×10^{-9}
0.0001	2.6×10^{-8}	4.9×10^{-12}

Evidently the MATHCAD programming is correct.

The zero-pressure surface and the potential on it, when the trough of the short wave coincides with the crest of the long wave, are suitable starting conditions for the exact computations. We can first check the same case of small ka , and compare with the results in Table 1. If the 2nd order potential is included in the calculation of the starting conditions, then the error when the computations had run until the crests coincided, was 2×10^{-9} at $ka = 0.001$. This is within the bounds of error of the result in Table 1, and compared with the crest elevation, it is 1 part in 10^6 .

3. RESULTS AND DISCUSSION

The exact computations were then run (again with 2nd order starting conditions) with much larger values of ka to find the point when the waves began to break. Figure 1 shows the results, together with the corresponding particle-sheet computations, using both the 1st order potential (2) and 1st + 2nd order potential (2) + (3), and starting the particles on the two different zero-pressure surfaces (both based on the full pressure formula).

As can be seen, the breaking thresholds are:

- $ka = 0.17$ with the 1st order potential
- $ka = 0.21$ with the 1st + 2nd order potential
- $ka = 0.18$ with the exact computations

These results are quite close – especially with the 1st order potential alone, when the threshold of “escape” differs from the breaking threshold by only about 5%.

The fact that the threshold of “escape” is higher when the 2nd order potential is included, is to be expected from the minus sign in (3). In the combined crest, when the crests of the two waves coincide, (i.e. $x = t = 0$ above), both the horizontal velocity $\partial\phi/\partial x$ and pressure $-\rho\partial\phi/\partial t$ are positive in (2), but both are negative in (3). So the action of the 2nd order potential is opposing that of the 1st order potential.

Figure 1 also reveals interesting differences in the position where the breaking occurs. The long wave overtakes the short wave at a speed $\sqrt{g/k_2} - \sqrt{g/k_1} = \sqrt{g}(1 - \sqrt{1/2})$ so the crests coincide after a time $(\pi/2)/\{\sqrt{g}(1 - \sqrt{1/2})\}$. Since the crests of the long wave are initially at $-\pi, \pi$, there will after that time be a crest of the long wave is at $-\pi + \sqrt{g}(\pi/2)/\{\sqrt{g}(1 - \sqrt{1/2})\} = \pi\{2(1 - \sqrt{1/2})^{-1} - 1\} = 2.221\text{m}$. This nominal focus point is shown in Figure 1 with an arrow – it is actually also the point of maximum crest elevation with classical 2nd order theory.

It is not surprising that the fully-nonlinear computations show the waves coming to a focus and breaking later, because it is well-known that steep focused waves in experiments do this, see e.g. Chaplin et al. [8]. More surprising is the way that the particle-sheet computations do this too, even though they are based on the ordinary potential (2) or (2) + (3), which show no such effect in the classically-defined surface. It is evidently not necessary to invoke the 3rd order effect of increasing wave speed with amplitude (see e.g. Newman [9] p. 249) to displace the focus point.

Figure 2 shows the effect in more detail (it includes a vertical scale exaggeration of 2:1), by comparing the successive stages in the 1st order particle-sheet computations for $ka = 0.16$, with the zero-pressure surfaces at the same times. It may be seen that the maximum crest elevation with the zero-pressure surfaces is reached precisely at the nominal focus point, as it should be. The crest elevation is incidentally 0.2639m, compared with the classically-defined crest elevation which from (1) is $0.16/2 + 0.16/1 = 0.24\text{m}$.

By contrast the particle-sheet surfaces reach their maximum crest elevation considerably later, and this elevation is greatly enhanced. This is because $ka = 0.16$ is only one step short of the particle “escape” at $ka = 0.17$, when the crest elevation becomes infinite.

As the wave steepness increases further, it may be seen in Figure 1 that the point of overturning moves back towards the focus point, just as it does with the fully-nonlinear computations. When the 2nd order potential is included, the particle-sheet reproduces the fully-nonlinear computations very well at $ka = 0.15$, but thereafter the results are generally worse. The “escape” occurs after the breaking, and its position jumps back to the other side of the nominal focus point.

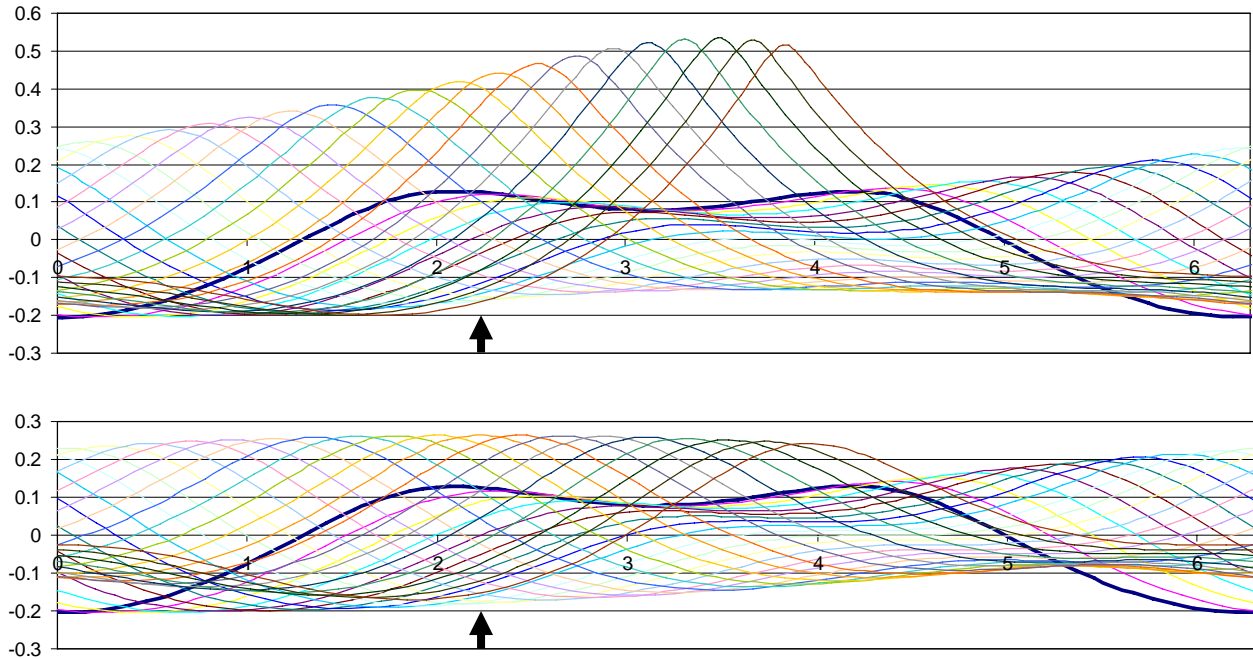


FIGURE 2. Particle-sheet surfaces (top) and constant-pressure surfaces (bottom), for the case $ka = 0.16$ in Figure 1. The bold line is the surface at the start of the computations, which is the same in both cases, and shows the crest of the long wave coinciding with the trough of the short wave. The other lines are the surface at successive intervals of 5% of the time until the crests coincide. 28 such successive surfaces are shown. Both graphs have a vertical scale exaggeration of 2:1, and the nominal focus point is shown with an arrow, as in Figure 1.

4. CONCLUSIONS

Overall, the particle-sheet computations reproduce the effect of breaking best when based simply on the 1st order potential, i.e. without including the 2nd order potential.

This is also more satisfactory from a logical point of view. Introducing the 2nd order potential delays the threshold of particle “escape” from $ka = 0.17$ to $ka = 0.21$. In the region between 0.17 and 0.21 there is a logical conundrum, because here the particle-sheet simulations are effectively relying on the 2nd order potential to prevent particle “escape”. Yet this second-order potential itself relies on an argument about the dynamic error on the first-order kinematically-exact surface (or vice-versa, as explained in Section 1). This argument breaks down when there is a particle “escape” in that 1st order kinematically-exact surface.

So it appears that the particle “escape” in the 1st order flow is the significant thing, and should be taken as the sign of wave breaking. The attraction of this view of wave breaking is of course its great simplicity. To detect breaking, it is merely necessary to track a single particle, in the way illustrated in Figure 2 in the author’s paper [1] at the 2002 Workshop.

However long the simulation, the particle cannot drift off vertically prior to “escape” because the 1st order flow has zero vertical velocity at great depth. By conservation of volume, it thus has zero vertical velocity, on average, at the surface too. Breaking statistics can therefore be established by long simulations in irregular waves – see [3].

REFERENCES

- [1] Rainey, R.C.T., 2002 “Escape” of particle trajectories in linear irregular waves: A new explanation for wave breaking and model of breaking waves. Proc. 17th IWWF, 155-158.
- [2] New, A.L., McIver, P. & Peregrine, D.H. 1985 Computations of overturning waves. JFM, **150** 233-251
- [3] Rainey, R.C.T., 2004 *An elementary theory of wave breaking* submitted to JFM.
- [4] Rainey, R.C.T. & Chaplin, J.R. 2003 *Waves breaking and cavitation around a vertical cylinder: experiments and linear theory*. Proc. 18th IWWF
- [5] Tulin, M.P. 2003 *Discussion of “Wave breaking and cavitation around a vertical cylinder in waves: experiments and linear theory.”* Proc. 18th IWWF
- [6] Dold, J.W. 1992 *An efficient surface-integral algorithm applied to unsteady gravity waves*. J. Computational Physics, **103** no.1, 90-115
- [7] Longuet-Higgins, M.S. & Stewart, R.W. 1960 *Changes in the form of short gravity waves on long waves and tidal currents*. JFM, **8** 565-583
- [8] Chaplin, J.R., Rainey, R.C.T. & Yemm, R.W. 1997 *Ringling of a vertical cylinder in waves* JFM, **350**, 119-147
- [9] Newman, J.N. 1978 *Marine Hydrodynamics*. MIT Press

Discussor: H. B. Bingham

Have you considered applying this idea to predict the breaking point of waves shoaling on a beach? It seems like it would be straightforward to do in the context of a mild slope and energy flux conservation.

Author's Reply:

That is an interesting suggestion. Howell Peregrine drew my attention to a paper by Biesel (U.S. National Bureau of Standards, Washington, Circular no. 521 (1952) 243-253) which does something similar on the assumption that the particles move in ellipses, as in a Gerstner wave. Biesel found that the surface particles began to overturn, at a certain point on the beach. I would presumably find the same. My argument is different, however, since I am not constraining the particles to move in ellipses (and I have no vorticity, unlike a Gerstner wave). Therefore I would presumably find a different breaking point. This point is discussed, together with many other results using my approach, in my paper in the Newman Honorary Volume of J. Eng. Maths. (to appear - 2007).